View metadata, citation and similar papers at core.ac.uk

brought to you by CORE

provided by Universiti Teknologi Malaysia Institutional Repository

JOURNAL OF APPLIED PHYSICS 103, 123520 (2008)

Thermomigration induced degradation in solder alloys

Cemal Basaran,[a] Shidong Li, and Mohd F. Abdulhamid
Electronic Packaging Laboratory, State University of New York at Buffalo, Buffalo, New York 14260-4300, USA

(Received 18 February 2008; accepted 15 April 2008; published online 19 June 2008)

Miniaturization of electronics to the nanoscale brings new challenges. Because of their small size and immense information and power processing capacity, large temperature gradients exist across nanoelectronics and power electronics solder joints. In this paper, a fully coupled thermomechanical-diffusion model is introduced to study the thermomigration induced strength degradation. A nonlinear viscoplastic material model with kinematic and isotropic hardening features is utilized. The model takes into account microstructural evolution of the material. A grain coarsening capability is built into the model to study its influence on thermomigration in solder alloys. The model is validated by comparing the simulation results with experimental data. © *2008 American Institute of Physics*. [DOI: 10.1063/1.2943261]

INTRODUCTION

The insatiable demand for higher performance and associated miniaturization of electronics progresses approximately according to Moore's law. Very-large-scale-integration (VLSI) interconnection sizes are continuously reduced accordingly to enable a higher degree of integration. By transmitting more data through smaller features, current density is increased significantly. Another byproduct of high current density in power electronic devices, especially SiC based devices that operate at high temperatures, is thermal gradient due to Joule heating. Both increased current density and temperature gradients pose major reliability concern especially for the solder joints of an electronic package. Because of their very low melting temperature, relative to service temperatures, solder alloys are susceptible to high diffusivity.[1–7]

Electromigration (EM) is a mass diffusion process as a result of an exchange of momentum between charge carrier free electrons and the ions of a conductor. When a metal is subject to a high current density, the so-called electron wind transfers part of the momentum to the atoms (or ions) of metal (or alloy), which make the atoms (or ions) move in the direction of the free electrons. EM causes atomic accumulation and hillock formation in the anode side and vacancy condensation and void formation in the cathode side.[4,5] Both hillocks and voids will cause degradation of the solder joint. However, failure is always observed on the void side.

The phenomenon of EM has been known for more than 100 years.[8] However, it became a concern only when the relatively severe conditions resulting from miniaturization of integrated circuits made it significant. EM occurs only when current density is above a certain threshold. The increase in the operating current inevitably causes the current density to be carried by each solder joint to rise dramatically too. Therefore, EM has become an inevitably critical reliability issue for solder joints.

Thermomigration (TM) is a mass transport caused by a large temperature gradient. If an initially homogeneous two-component alloy is placed within a temperature gradient, above a critical level, mass diffusion can lead to disintegration of the components. One constituent diffuses faster to the cold side, and as a result the hot region becomes depleted in that component. This effect is known as the Soret effect (also Ludwig–Soret effect) in fluids.[9] This resulting diffusion process is known as TM or thermal diffusion.

Historically, the influence of TM on EM has been ignored. This is perhaps because of the assumption that the magnitude of TM flux is much smaller than EM. Recently scientists theoretically and experimentally have shown that when the thermal gradient is large enough, the TM can be the dominant migration process.[1,3,4,10] Ye *et al.*[4] was the first to show that TM forces can be larger than EM forces in flip chip solder joints.

In this study, TM effects on lead-free solder joints are studied both numerically and experimentally. In order to achieve this objective, a fully coupled thermomechanical-diffusion analysis is performed with a viscoplastic nonlinear material model that accounts for microstructural evolution of the material. High thermal gradients, as high as $1000\ ^\circ\mathrm{C/cm}$, are applied to SnAgCu solder joints without any current flow. In other words, samples in our experiment are solely subjected to high temperature gradients but no electrical current in order to study influence of thermal gradient (and associated TM) without interference from EM and Joule heating. The vacancy evolution, grain coarsening, and hardening effects are studied by finite element method. The numerical results are verified by experimental data.

GOVERNING EQUATIONS

Under high temperature gradients, mass/vacancy diffusion is driven by three forces.

(1) *Thermal gradient*. Joule heating generated under the conditions of a high electricity current density is highly localized and consequently results in a thermal gradient in the medium, which leads to TM.

[a]Author to whom correspondence should be addressed. Electronic mail: cjb@buffalo.edu.

© 2008 American Institute of Physics

Downloaded 25 Nov 2008 to 128.205.55.15. Redistribution subject to AIP license or copyright; see http://jap.aip.org/jap/copyright.jsp

(2) Stress gradient is another driving force of mass transport. There is a strong interaction between the stress gradient and the other driving forces. Stress gradient can counteract or enhance the migration process.[11–19] However, in the absence of an external stress gradient, as the mass moves from the hot side to cold side, compression on the cold side and tension on the hot side develops, which counters the thermal gradient induced force.
(3) The atomic vacancy concentration gradient, which is usually small at the beginning compared to the former two items,[1] however, as the mass migration progresses, vacancy concentration gradient increases significantly between the hot side and cold side.

Mass diffusion

TM is a diffusion controlled mass transport process. It is governed by the following vacancy conservation equation that is equivalent to the mass conservation equation:

$$C_{V0}\frac{\partial c}{\partial t} + \nabla \mathbf{q} - G = 0, \tag{1}$$

where C_{V0} is the equilibrium vacancy concentration in the absence of a stress field, c is the normalized vacancy concentration and $c = C_V/C_{V0}$, C_V is the vacancy concentration, t is the time, and $\mathbf{q}$ is the vacancy flux,[1,20,21]

$$\mathbf{q} = -D_V C_{V0}\left[\nabla c + \frac{c}{kT^2}Q^* \nabla T + \frac{cf\Omega}{kT}\nabla \sigma^{\mathrm{sp}}\right] \tag{2}$$

where D_V is the effective vacancy diffusivity, f is the vacancy relaxation ratio, ratio of atomic volume to the volume of a vacancy, Ω is the atomic volume, k is Boltzmann's constant, T is the absolute temperature, σ^{sp} is the spherical part of stress tensor, $\sigma^{\mathrm{sp}} = \mathrm{tr}(\sigma_{ij})/3$, and Q^* is the heat of transport, the isothermal heat transmitted by moving the atom in the process of jumping a lattice site less the intrinsic enthalpy. G is the vacancy generation/annihilation rate

$$G = -C_{v0}\frac{c - \exp\left[\dfrac{(1-f)\Omega\sigma^{\mathrm{sp}}}{kT}\right]}{\tau_s}. \tag{3}$$

τ_s is the characteristic vacancy generation/annihilation time.

Force equilibrium

Continuum mechanics equilibrium is given by

$$\nabla \sigma + f = 0. \tag{4}$$

In this study we are primarily interested in solder joints. Because most electronic solder alloys are above $0.6T_m$ (T_m: melting temperature), in room temperature, viscoplasticity must be considered in the nonlinear material model. As a result the material model must be a coupled thermomechanical-diffusion model.

The strain-stress constitutive model is established as

$$\sigma = \Box(\varepsilon,\dot{\varepsilon}) \cdot (\boldsymbol{\varepsilon}_{\mathrm{tot}} - \boldsymbol{\varepsilon}_{\mathrm{viscoplastic}} - \boldsymbol{\varepsilon}_{\mathrm{diffusion}} - \boldsymbol{\varepsilon}_{\mathrm{thermal}}), \tag{5}$$

where $\varepsilon_{\mathrm{tot}}$ is the total strain, $\varepsilon_{\mathrm{viscoplastic}}$ is the strain due to viscoplastic deformation, $\varepsilon_{\mathrm{diffusion}}$ is the strain due to TM, $\varepsilon_{\mathrm{thermal}}$ is the strain due to thermal expansion, and $\Box(\varepsilon,\dot{\varepsilon})$ is the tangential constitutive tensor.

Heat transfer

The basic heat transfer equation is given by

$$\rho C_p \frac{\partial T}{\partial t} - \nabla(k_h \nabla T) - \rho Q = 0, \tag{6}$$

where ρ is the density of the material, C_p is the specific heat k_h is the coefficient of heat transfer, and Q is the heat generated within the body, which can be decomposed into two components,

$$Q = Q_P + Q_V. \tag{7}$$

where Q_P is the heat generated by plastic deformation at step $n+1$ described as

$$Q_P = \sigma_{n+1}:\dot{\varepsilon}^{\mathrm{vp}}_{n+1}, \tag{8}$$

where $\dot{\varepsilon}^{\mathrm{pl}}$ is the plastic strain rate. Q_V is the heat generated due to vacancy flux, which can be expressed by

$$Q_V = \mathbf{q}:F_k, \tag{9}$$

where $\mathbf{q}$ is the vacancy flux as shown in Eq. (2) and F_k is the effective driving force which has the form of

$$F_k = -\left(f\Omega \nabla \sigma^{\mathrm{sp}} + \frac{Q^*}{T}\nabla T + \frac{kT}{c}\nabla c\right). \tag{10}$$

Because ABAQUS and all other commercially available general purpose finite element codes do not have the capability to solve the nonlinear TM problem directly with nonlinear material properties that account for microstructural evolution, the governing equations above are implemented by exploiting ABAQUS user element (UEL) and user material (UMAT) features.

VISCOPLASTICITY MODEL

The strain-stress constitutive model in the absence of viscosity is established as

$$\boldsymbol{\sigma} = \Box(\boldsymbol{\varepsilon}_{\mathrm{tot}} - \boldsymbol{\varepsilon}_{\mathrm{viscoplastic}} - \boldsymbol{\varepsilon}_{\mathrm{diffusion}} - \boldsymbol{\varepsilon}_{\mathrm{thermal}}), \tag{11}$$

where

$$\Box = \kappa \mathbf{1} \otimes \mathbf{1} + 2\mu\left(\mathbf{I} - \tfrac{1}{3}\mathbf{1} \otimes \mathbf{1}\right),$$

κ is the bulk modulus, and μ is the shear modulus,

$$\mathbf{1} = \begin{bmatrix} 1 & 0 & 0 & 0 & 0 & 0 \\ 0 & 1 & 0 & 0 & 0 & 0 \\ 0 & 0 & 1 & 0 & 0 & 0 \\ 0 & 0 & 0 & 0 & 0 & 0 \\ 0 & 0 & 0 & 0 & 0 & 0 \\ 0 & 0 & 0 & 0 & 0 & 0 \end{bmatrix}, \quad \mathbf{1} = \begin{bmatrix} 1 \\ 1 \\ 1 \\ 0 \\ 0 \\ 0 \end{bmatrix}.$$

Itemized strain components can be simplified as follows:

Downloaded 25 Nov 2008 to 128.205.55.15. Redistribution subject to AIP license or copyright; see http://jap.aip.org/jap/copyright.jsp

$$\boldsymbol{\varepsilon}_{\rm tot} = \frac{1}{3}\boldsymbol{\varepsilon}_{\rm tot}^{\rm trace} \cdot \mathbf{1} + \boldsymbol{\varepsilon}_{\rm tot}^{\rm dev}, \quad (12)$$

$$\boldsymbol{\varepsilon}_{\rm viscoplastic} = \tfrac{1}{3}\boldsymbol{\varepsilon}_{\rm viscoplastic}^{\rm trace} \cdot \mathbf{1} + \boldsymbol{\varepsilon}_{\rm viscoplastic}^{\rm dev} = \boldsymbol{\varepsilon}_{\rm viscoplastic}^{\rm dev}, \quad (13)$$

$$\boldsymbol{\varepsilon}_{\rm diffusion} = \tfrac{1}{3}1 \cdot \boldsymbol{\varepsilon}_{\rm diffusion}^{\rm trace}, \quad (14)$$

$$\boldsymbol{\varepsilon}_{\rm thermal} = \alpha(T - T_0) \cdot \mathbf{1}, \quad (15)$$

where $\boldsymbol{\varepsilon}_{\rm diffusion}^{\rm trace}$ must be defined at the atomic lattice level by the following equation:[20]

$$\frac{\partial \boldsymbol{\varepsilon}_{\rm diffusion}^{\rm trace}}{\partial t} = \Omega C_{v0}\left(f\nabla \mathbf{q} + f'\frac{G}{C_{v0}}\right), \quad (16)$$

where $f' = 1 - f$, which is the volumetric strain at an atomic lattice site due to a vacancy. In TM induced mass transport, it is assumed that when an atom vacates a site, due to the difference between the volume of an atom and the volume of a vacancy, spherical lattice strain is exerted. This spherical strain, however, leads to shear strain due to geometric boundary conditions.

Using Eq. (1), we can transform Eq. (16) into

$$\frac{\partial \boldsymbol{\varepsilon}_{\rm diffusion}^{\rm trace}}{\partial t} = \Omega C_{v0}\left(\frac{G}{C_{v0}} - f\frac{\partial c}{\partial t}\right) = \Omega C_{v0}\left[\frac{e^{(1-f)\Omega\sigma_{\rm spherical}/kT} - c}{\tau_s} - f\frac{\partial c}{\partial t}\right]. \quad (17)$$

Highly viscoplastic behavior with nonlinear kinematic/isotropic hardening has been observed in microelectronic solder joints.[5] Hence, a rate dependent combined isotropic-kinematic hardening model is introduced in this paper to consider the plastic deformation of solder material. Yield function is defined by[22,23]

$$\mathbf{F} = \|\boldsymbol{\xi}\| - \sqrt{\tfrac{2}{3}}K(\alpha), \quad (18)$$

where $\boldsymbol{\xi}$ is the relative deviatoric stress tensor defined by $\boldsymbol{\xi} = \mathbf{s} - \mathbf{X}$. $\mathbf{s}$ is the deviatoric stress tensor and $\mathbf{X}$ is the back stress tensor whose evolution is given by the following equation:

$$\frac{\partial \mathbf{X}}{\partial t} = c_1\dot{\boldsymbol{\varepsilon}}^{\rm vp} - c_2\mathbf{X}\dot{\alpha}, \quad (19)$$

where c_1 is linear kinematic hardening constant and c_2 is the nonlinear kinematic hardening constant.

$K(\alpha)$ represents the isotropic hardening component defining the radius of the yield surface in stress space. It is a function of the equivalent plastic strain α given by

$$K(\alpha) = \sqrt{\frac{2}{3}}\sigma_y + R_\infty[1 - e^{-c\alpha}], \quad (20)$$

where Y_0 is the initial yield stress, R_∞ is the isotropic hardening saturation value, c is the isotropic hardening rate, α is the equivalent plastic strain given by $\alpha = \int\sqrt{\tfrac{2}{3}\dot{\varepsilon}_{ij}^{p}\dot{\varepsilon}_{ij}^{\rm vp}}dt$, and

$$\dot{\alpha} = \sqrt{\tfrac{2}{3}}\gamma, \quad (21)$$

where γ is the consistency parameter.[19]

CREEP MECHANISM

Grain boundaries play an important role in solder alloy creep mechanism, which is dominated by a slip and glide process,[22–24] which happens when a shear stress acts on the grain boundary plane and causes the grains to slide and glide. This means that fine-grained solder alloys have a poor resistance to creep relative to coarser grained ones, especially at high temperatures. In this study, this mechanism is considered to be the dominant one for the primary and steady states by the viscoplastic model given by Eq. (22).

The viscoplastic model adopted in this paper is the flow rule for solder alloys, which was developed by Basaran and co-workers[12,23,25] based on the Kashyap and Murty model.[26] In this model, grain boundary sliding is the dominant creep mechanism. Primary and steady state creeps can be given by

$$\dot{\varepsilon}_{ij}^{\rm vp} = \frac{AD_0Eb}{k\theta}\left(\frac{\langle F\rangle}{E}\right)^n\left(\frac{b}{d}\right)^p e^{-Q/RT}\frac{\partial \mathbf{F}}{\partial \sigma_{ij}}, \quad (22)$$

where the material parameters are defined as follows: A is a dimensionless material parameter to describe the strain rate sensitivity. $D_0e^{(-Q/R\theta)}$ is a diffusion coefficient, in which D_0 is a frequency factor, Q is the creep activation energy for viscoplastic flow, R is the universal gas constant $= 8.314$ J/K mol$= 8.314$ N mm/K mol, T is the absolute temperature in Kelvin, E is Young's modulus, b is the characteristic length of crystal dislocation (magnitude of Burger's vector), k is Boltzmann's constant, d is the average phase size (which will be discussed below), p is the phase size exponent, and n is the stress exponent for plastic deformation rate, where $1/n$ indicates strain rate sensitivity.

GRAIN SIZE EFFECTS

Basaran and Wen[29] have shown that most electronic solder alloys are in thermodynamically unstable state as flown. Their microstructure and properties evolve during service. It is well known that[24–29] the average grain size gets larger under thermal loading. The microstructural coarsening is recognized as one of the most serious problems for solder joint reliability.

The phase growth model adopted in this paper was suggested by Sayama *et al.*,[28]

$$\Delta S = \Delta S_t + \Delta S_c, \quad (23)$$

where ΔS is the phase growth parameter increment defined by $S = d^4$. ΔS_t is the thermal equilibrium phase growth parameter increment given by

$$\Delta S_t = C_1\Delta t, \quad (24)$$

where C_1 is a temperature dependent material parameter, for solder,[27] which has a form of

$$C_1 = 2.16 \times 10^4 \exp(-6.33 \times 10^3/T). \quad (25)$$

ΔS_c is the strain induced phase growth parameter increment with the form of

$$\Delta S_c = C_2\dot{\varepsilon}_c\Delta t, \quad (26)$$

where $\dot{\varepsilon}_c$ is the equivalent creep strain rate and C_2 is another material parameter[27] given by

Downloaded 25 Nov 2008 to 128.205.55.15. Redistribution subject to AIP license or copyright; see http://jap.aip.org/jap/copyright.jsp

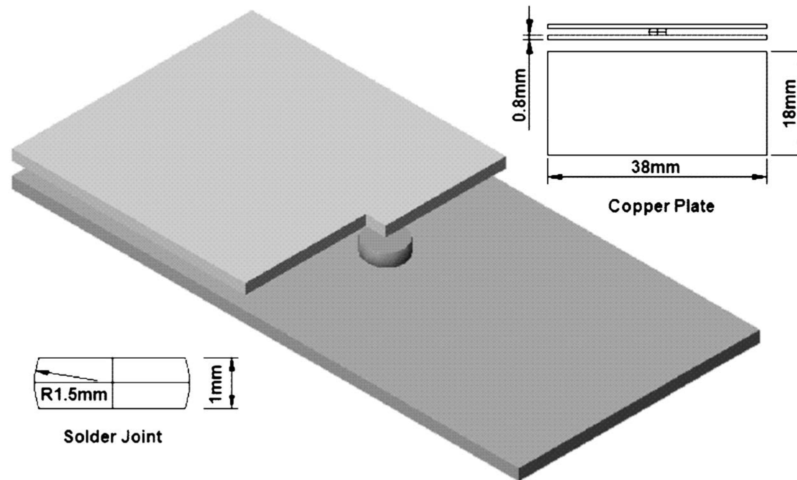

FIG. 1. Geometry of the test vehicle.

$$C_2 = 6.51 \times 10^2 \exp(6.29 \times 10^2/T). \tag{27}$$

In this paper, microstructural evolution [Eq. (23)] has been taken into consideration in the following three processes: effective diffusivity [Eq. (28)], creep mechanism [Eq. (22)], and yield strength [Eqs. (18) and (30)]. We believe that this is necessary because as flowed, solder joints are not in thermodynamically stable state. Their low melting temperature allows them to easily reduce the grain boundary surface area by coarsening to reach a lower surface energy level.

Effective diffusivity

The net mass transport in TM is a result of lattice diffusion and grain boundary diffusion. Surface diffusion in solder joints is relatively small compared to other mechanics. However, the same cannot be said for VLSI interconnects. To account for both mechanisms, Hart[30] has suggested a grain size dependent apparent diffusivity given by

$$D_a = D_L + (\delta/d)D_{gb}, \tag{28}$$

where D_a is the effective atomic diffusivity, D_L is the lattice diffusivity, D_{gb} is the grain boundary diffusivity, and (δ/d) represents the fraction of atoms in grain boundaries. Singh[31] also showed that at high temperatures $(\delta/d)D_{gb} \gg D_L$. He suggested that Hart's model can be simplified by ignoring the lattice diffusion because grain boundary diffusivity is larger by an order of magnitude,

$$D_a = (\delta/d)D_{gb}. \tag{29}$$

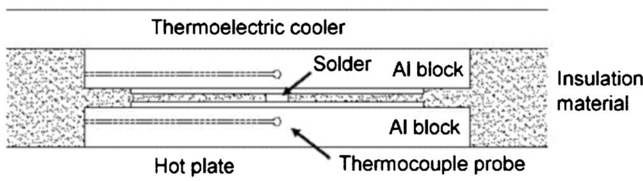

FIG. 2. Front view of the test vehicle.

Yield strength

The dependence of the yield stress on grain size in metals is well known.[32] It follows that yield stress decreases with the coarsening of the grain size. The phenomenon is generally explained by the grain boundary strengthening theory. The lattice structures of adjacent grains differ in orientation. Therefore it requires more energy for a dislocation motion to change direction and move from one grain into the adjacent grain, which has a different crystallographic orientation. Impeding this dislocation motion hinders the initiation of the slip process and thus increases the yield strength of a material.

Several models have been proposed to describe this relationship[32–34] in different materials. In a recent publication,[35] Siviour *et al.* illustrated the mechanical properties of solder alloys by showing that the dependence of strength on strain rate for 96.5%Sn–3.5%Ag is much smaller compared with that for SnPb solder. The latter follows a Hall–Petch style relationship under a given strain rate. Hence in our study, the grain size dependence of the material strength relationship based on the Hall–Petch model is given by

$$\sigma_y = \sigma_0 + k_1 d^{-1/2} + k_2 T, \tag{30}$$

where σ_y is the yield stress, σ_0 is the Hall–Petch constant that represents the internal resistance to the motion of a dislocation through the crystal lattice and that is approximately

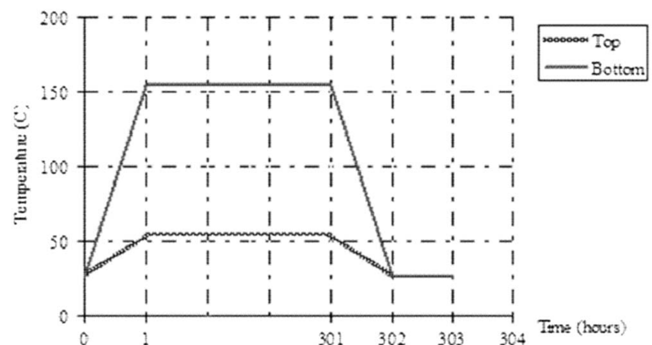

FIG. 3. Thermal loading profile.

Downloaded 25 Nov 2008 to 128.205.55.15. Redistribution subject to AIP license or copyright; see http://jap.aip.org/jap/copyright.jsp

TABLE I. Material properties for SAC405 used in this paper.

Item	UNIT	SAC405
Vacancy relaxation time (TS)	s	1.80×10^{-3} [a]
Diffusivity(D)	$\mu m^2\ s^{-1}$	2.722×10^{10} [b]
Resistivity	$\mu m^3\ S^{-3}\ A^{-2}$ Kg	$1.52\times10^{11}+3.50\times10^{8}T$
Average vacancy relaxation ratio (F)	N/A	0.2 [a]
Atomic volume (Ω)	μm^{-3}	2.71×10^{-11} [b] (pure tin)
Vacancy concentration at stress free state (C_{V0})	μm^{-3}	1.107×10^{6} [c]
Young modulous cons	Kg s μm^{-1}	$5.77\times10^{4}-56.4T$ [d]
Poisson ratio	N/A	0.33 [d]
Initial yield stress	Kg s μm^{-1}	$79.98+95/\sqrt{d}-0.2133T$ [e]
Coefficient of thermal expansion (CTE)	K^{-1}	18.9×10^{-6} [f]
Linear kinematic hardening cons (XINFI)	Kg s μm^{-1}	9.63×10^{3} [g]
Nonlinear kinematic hardening cons (GAMHARD)	Kg s $K^{-1}\ \mu m^{-1}$	7.25×10^{2} [g]
Isotropic hardening rate (CHARDI)	N/A	3.83×10^{2} [g]
Dimensionless cons (A)	N/A	7.60×10^{9} [g]
Burgers vector (B)	μm	3.18×10^{-4} [h] (for pure tin)
Initial average grain size	μm	2.45 [e]
Grain size exponent	N/A	3.34 [i]
Stress exponent	N/A	6.65 [d]
Creep activation energy	$\mu m^2\ s^{-2}$ Kg mol^{-1}	7.95×10^{16} [d]
Heat of transport ($Q*$)	Kg $\mu m^2\ s^{-2}$	-3.68×10^{-8} [j]
Activation energy	$\mu m^2\ s^{-2}$ Kg	4.895×10^{16} [b]
Density	Kg μm^{-3}	7.39×10^{15} [k]
Specific heat	$\mu m^2\ s^{-2}\ K^{-1}$	2.19×10^{14} [l]
Heat conductivity	Kg $\mu m\ s^{-3}\ K^{-1}$	5.73×10^{7} [m]

[a] Reference 21.
[b] Reference 7.
[c] References 7 and 38.
[d] Reference 39.
[e] Reference 35.
[f] Reference 40.
[g] Reference 41.
[h] Reference 42.
[i] Reference 26.
[j] Reference 43.
[k] Reference 44.
[l] Reference 45.
[m] Reference 46.

the yield stress of a single crystal, k_1 is a constant considering the impeding effect of grain boundaries on dislocation, and k_2 is a constant showing the dependence of strength on temperature.

EXPERIMENTAL SETUP

The test vehicle is illustrated in Fig. 1. The lead-free solder alloy used in this study is commercially available and

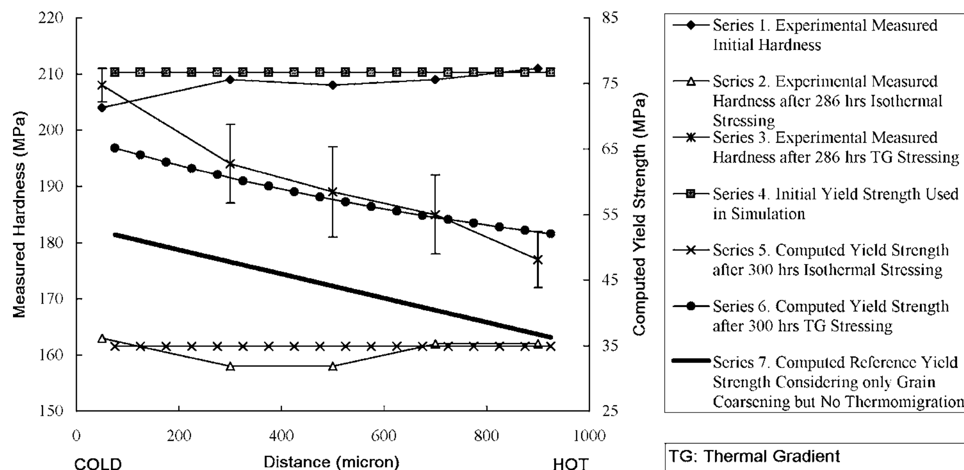

FIG. 4. Comparison of the yield strength calculated with measured hardness.

Downloaded 25 Nov 2008 to 128.205.55.15. Redistribution subject to AIP license or copyright; see http://jap.aip.org/jap/copyright.jsp

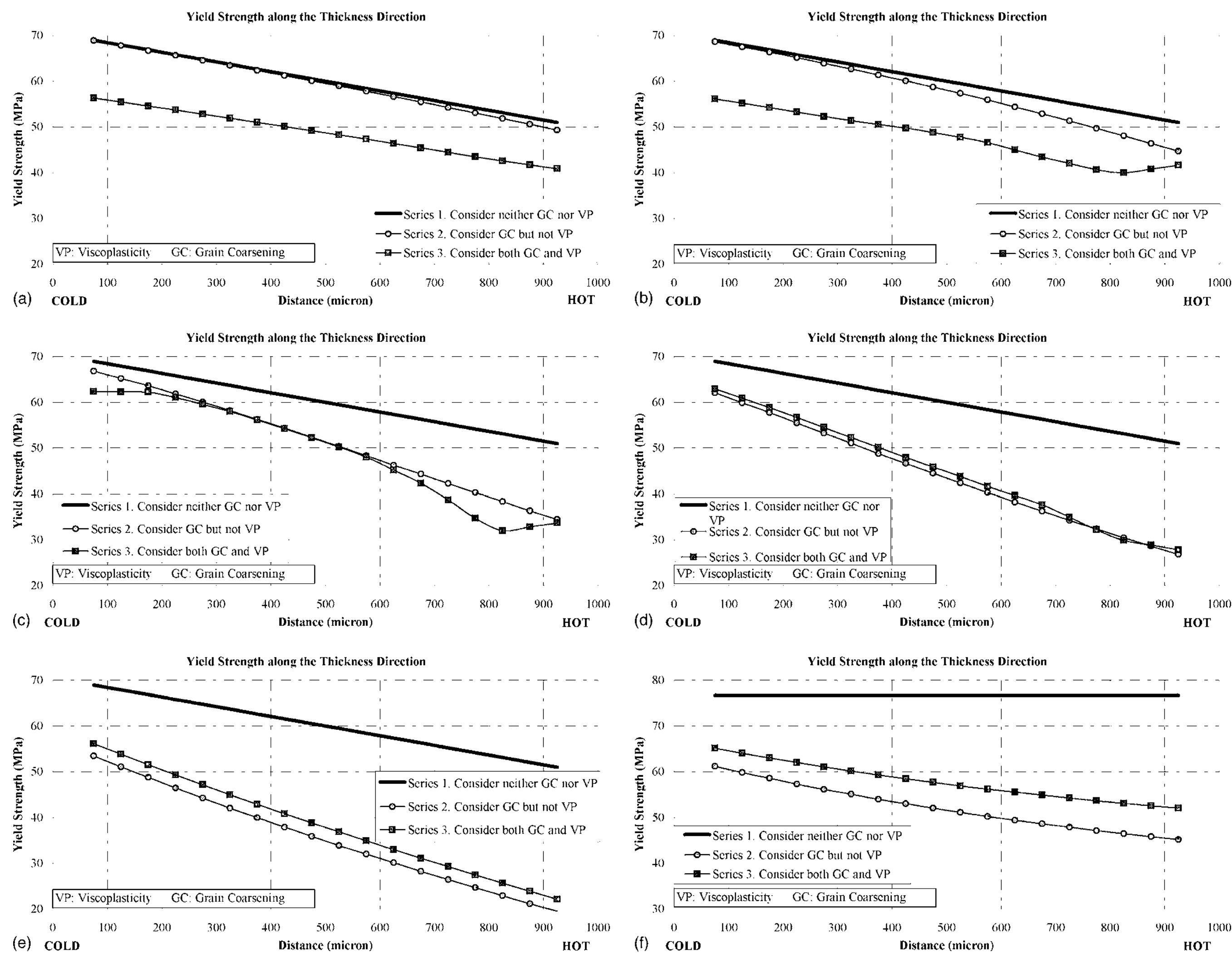

FIG. 5. Evolution of yield strength along the height of the solder joint.

is composed of 95.5%Sn, 4.0%Ag, and 0.5%Cu (SAC 405). The solder ball joins two copper plates with dimensions of 18×38 mm^2 and 0.8 mm thick.

The samples are sandwiched between a lower Al block in contact with a hot plate and an upper Al block in contact with a thermoelectric cooler, as shown in Fig. 2. Every contact surface is coated with thermal grease to maximize heat transfer. The open area between plates and between blocks is insulated to minimize heat radiation and circulating heat flow. The hot side and cold side temperatures are monitored with thermocouples and maintained at 160 and 50 °C, respectively, with a margin error of ±1 °C. Due to the small size of solder joints and the associated difficulty in measuring the temperature at the top and bottom of the solder joint, a heat transfer analysis was done using ABAQUS standard in order to get the temperature field in the solder ball. In the finite element analysis (FEA) heat transfer analysis, thermocouple reading temperatures are used as boundary conditions. The FEA results show that in the top and bottom of the solder joint, temperatures are 155 and 55 °C, respectively, thus creating a temperature gradient of 1000 °C/cm, which is large enough to induce TM in solder alloy.

FINITE ELEMENT SIMULATIONS

The proposed model is implemented in the ABAQUS general purpose finite element program using thermal-displacement analysis option. ABAQUS cannot solve the coupled thermomechanical-diffusion problem directly with nonlinear material models. By treating ABAQUS as a partial differential equation solver, we embedded the governing equations into an ABAQUS user element interface (UEL) after discretization for finite element method implementation. The viscoplastic material behavior, rate dependent coupled isotropic and kinematics hardening model,[20] and grain coarsening related effects are all implemented into an ABAQUS user material interface (UMAT).

In this simulation, eight-noded quadratic plane strain elements are used to simulate the TM process. At each node four degrees of freedom are utilized: two for displacements in the x and y directions, one for normalized vacancy concentration, and one for temperature. By taking into consideration that all the mechanical property measurements are done in the room temperature, a warming up stage and a cooling down stage are added before the thermal gradient stressing

Downloaded 25 Nov 2008 to 128.205.55.15. Redistribution subject to AIP license or copyright; see http://jap.aip.org/jap/copyright.jsp

phase and after it. Thermal loadings at the top and the bottom of solder bump are shown in Fig. 3. All the material properties used in this study are list in Table I.

RESULTS AND DISCUSSION

The hardness of a virgin SAC405 solder joint is measured in room temperature, shown in series 1 in Fig. 4. The samples are annealed in a thermal chamber at 170 °C (443 K) for 286 h. After annealing the samples are sectioned and the hardness along the solder height is measured, which is shown in series 2 in Fig. 4. By comparing series 1 and 2, it can be seen that the hardness reduces uniformly and significantly. The major reason for the hardness reduction is the grain growth during the heat treatment process. As we know, the coarsening of the grain leads to the decrease of yield stress, which has a positive correlation with the hardness modulus.[36]

Hardness measurements were conducted by MTS Nanoindenter with Berkovitch tip using continuous stiffness measurement features. Details of this process for solder alloys was discussed in Ref. 37.

To simulate the same heat treatment process, a uniformly distributed temperature is applied to the whole section using ABAQUS, which starts with room temperature (300 K) and gradually rises up to 170 °C (443 K) in 1 h as the warming process in our experiments; after that, temperature across the whole solder ball is kept at 170 °C (443 K) for 300 h; it follows by a 1 h ramp to cool the solder to room temperature (300 K) and keeps at 300 K for another 1 h to avoid probable fluctuations. The residual yield strength across the height of the solder is depicted as series 5 in Fig. 4. By comparison with the initial yield strength we used in this paper,[35] as can be seen from series 4 in Fig. 4, we can see that the annealing effect is well simulated with the model.

Series 3 in Fig. 4 shows the mean hardness and their 1 sigma error range as measured from four samples versus distance from the cold side (top side) to hot side (bottom side). All four samples have been subjected to a temperature gradient of 1000 °C/cm for 286 h before they are sectioned to measure hardness. It can be observed from series 3 that the hardness shows an increasing trend from the hot side to cold side. This differential hardness degradation is attributed to the effect of grain coarsening.

When TM effect is taken into account with microstructural considerations, simulation produces results much closer to the experimental data, as plotted in series 6 in Fig. 4. Figure 4 series 7 curve shows the variation of yield stress across the solder joint in the absence of TM forces with an elastic-perfectly plastic material model. From the difference between series 6 and series 7, we can see that the shift of yield surface is the result "hardening" due to the TM induced stress which exceeds the yield stress. In other words, we observe that TM induced stress is high enough to create a significant inelastic deformation and associated hardening.

Figure 5 shows the evolution of hardening /softening along the height of the solder joint with respect to the stressing time. The same information is presented in Fig. 6 using contours in the solder joints. In Fig. 5, series 1, we only

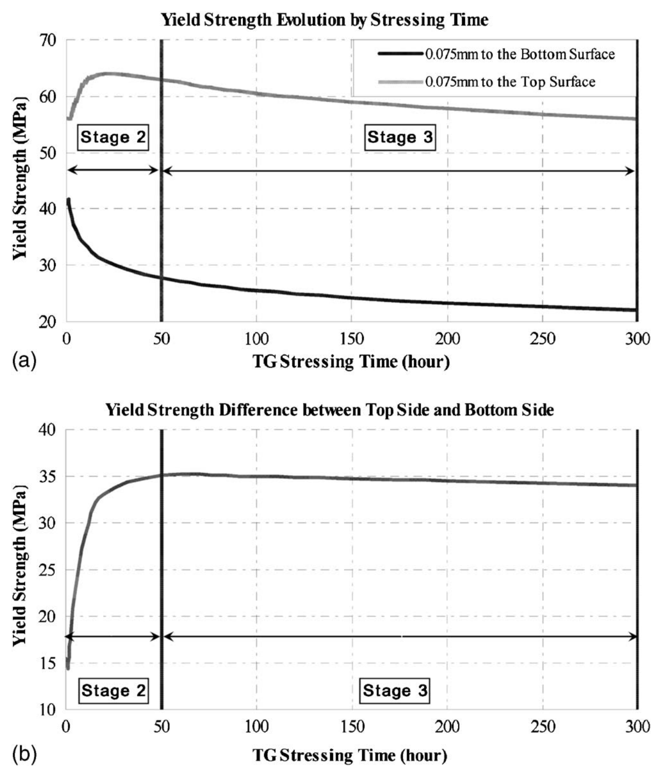

FIG. 6. Yield strength evolution contour map.

consider the temperature dependence of the yield strength but ignore the grain coarsening and viscoplasticity effects. We observe that the yield strength remains constant during the thermal gradient (TG) stressing. Figure 5(f) shows that after cooling down, yield strength increases, which is expected. In Fig. 5, series 2 curves, the variation of yield strength with respect to grain size is considered but not viscoplasticity. As can be observed in these curves, the yield strength gradually degrades during TG stressing. This relative degradation between the hot side and cold side is an irreversible process. After cooling down, yield strength increases along the height of the solder joint. However, the yield strength in the hot side is much smaller than that in the cold side because of the mass transport from the hot side to cold side. In Fig. 5, series 3 curve depicts the data where grain coarsening and TM induced viscoplasticity are both taken into consideration. In Fig. 4 we had shown that when both microstructural evolution and viscoplasticty are considered in the simulation, the results were closer to the experimental measurements. In Fig. 5 the difference between series 3 and series 2 curves is due to the inclusion of viscoplasticity in series 3. From Figs. 4 and 5, we can state that both grain coarsening and viscoplastic deformation happen during the TM. Grain coarsening keeps softening the material, while the viscoplastic strain makes the solder material to soften first and then harden. Therefore, any model for solder alloy TM must include both grain coarsening and viscoplasticity.

We should point out that on the cold side, experimentally measured hardness after 286 of TG is far off from computationally simulated yield stress. We believe that this is due to our model's weakness in handling mass immigration induced hardening in the cold side. In the future models, we intend to

Downloaded 25 Nov 2008 to 128.205.55.15. Redistribution subject to AIP license or copyright; see http://jap.aip.org/jap/copyright.jsp

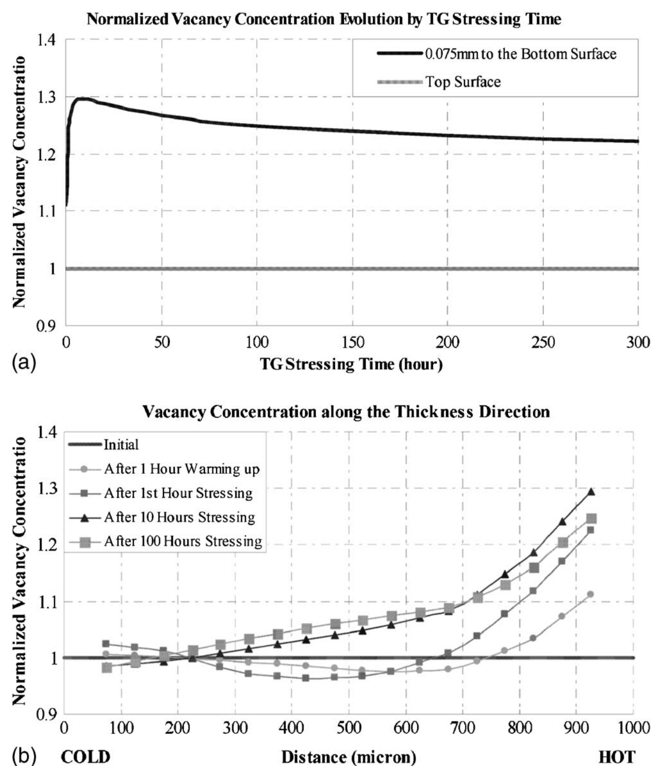

FIG. 7. Yield strength evolution by TG stressing time.

increase hardness as a function of increase in density, which may give us a better estimate on the cold side. However, because the failure always initiates at the hot side, we have not given the same attention to what happens at the cold side.

Figure 7 shows the yield strength evolution as a function of time during TM experiment. The cold side yield stress first increases, however, as time passes, the yield strength decreases; however on the hot side, decrease in yield stress starts from the beginning and continues during the experiment.

Figure 8(a) shows the evolution of the normalized vacancy concentration in the middle of the hot side as a function of TG stressing time. It can be observed that vacancy accumulates very fast at the first few hours until the three driving forces balance each other. Mass transport creates a large stress gradient and a large concentration gradient, which act opposite to the TG driving force. This results in a relaxation of vacancy concentration gradient. However, a highly concentrated vacancy can still be observed after 300 h of relaxation due to large thermal gradient. Figure 8(b) shows the vacancy distribution along the height of the solder joint in different stages of TM testing.

CONCLUSIONS

A fully coupled thermomechanical-diffusion model with nonlinear material properties is introduced to study the TM phenomenon. In order to understand the TM process clearly and in depth, EM is not included. A nonlinear kinematic/isotropic hardening viscoplasicity model and grain coarsening model are taken into consideration. By comparing the simulation results with experimental data, the model has been validated.

Grain coarsening effect plays an important role in TM related phenomenon. Grain size influences TM in three major aspects. (1) Grain size is an important factor for mass diffusion rate. The smaller the grain size is, the faster the diffusion is. This is probably because of the high grain boundary surface energy. (2) The creep rate for solder alloys

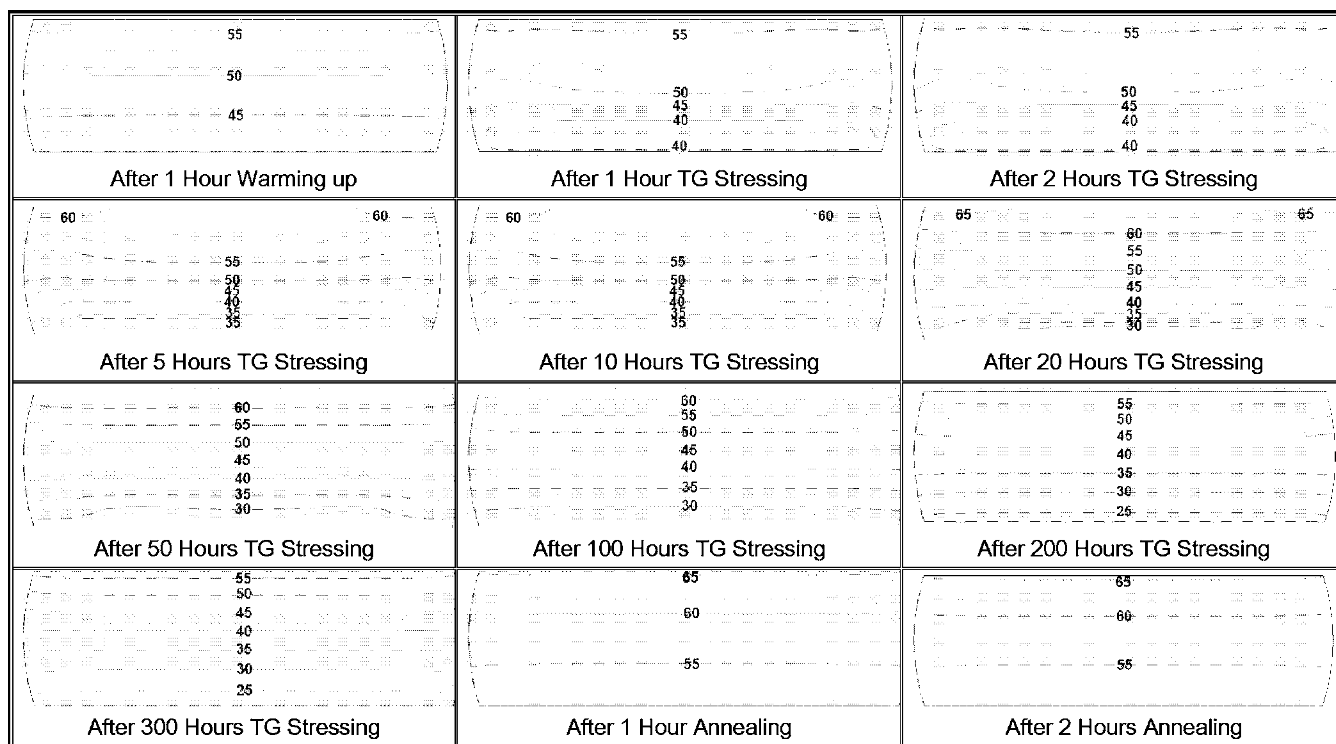

FIG. 8. Normalized vacancy evolution with TG stressing time.

Downloaded 25 Nov 2008 to 128.205.55.15. Redistribution subject to AIP license or copyright; see http://jap.aip.org/jap/copyright.jsp

highly depends on the grain size. (3) It has been shown that solder alloys strongly follow the Hall–Petch relationship during TM, which means that yield strength degrades with the grain growth.

In this study, it is observed that the softening due to grain coarsening is not the only mechanism that determines degradation of the hardness during TM. It is shown that viscoplasticity and microstructural evolution both must be considered in the model. An important finding of this paper is that TM induced stresses are well above the yield stress. The discrepancies between the numerical simulation results and experimental data on the cold side could be due to poor modeling of the influence of the mass condensation on material yield strength.

ACKNOWLEDGMENTS

This project has been sponsored by US Navy, Office of Naval Research, Advanced Electrical Power Systems program under the direction of Terry Ericsen. Guidance received from Terry Ericsen during the course of the project is greatly appreciated.

[1]C. Basaran, M. Lin, and H. Ye, Int. J. Solids Struct. **40**, 7315 (2003).
[2]C. Basaran, H. Ye, D. C. Hopkins, D. Frear, and J. K. Lin, J. Electron. Packag. **127**, 157 (2005).
[3]A. T. Huang, A. M. Gusak, K. N. Tu, and Y.-S. Lai, Appl. Phys. Lett. **88**, 141911 (2006).
[4]H. Ye, C. Basaran, and D. Hopkins, Appl. Phys. Lett. **82**, 1045 (2003).
[5]H. Ye, C. Basaran, and D. C. Hopkins, Int. J. Solids Struct. **40**, 4021 (2003).
[6]H. Ye, D. C. Hopkins, and C. Basaran, Microelectron. Reliab. **43**, 2021 (2003).
[7]H. Ye, "Mechanical behavior of microelectronics and power electronics solder joints under high current density: Analytical modeling and experimental investigation," Ph.D. thesis, State University of New York at Buffalo, 2004.
[8]F. Skaupy, Verh. Dtsch. Phys. Ges. **16**, 156 (1914).
[9]J. K. Platten, J. Appl. Mech. **73**, 5 (2006).
[10]C. Q. Ru, J. Mater. Sci. **35**, 5575 (2000).
[11]M. Shatzkes and Y. Huang, J. Appl. Phys. **74**, 6609 (1993).
[12]K. N. Tu, Phys. Rev. B **45**, 1409 (1992).
[13]I. A. Blech and C. Herring, Appl. Phys. Lett. **29**, 131 (1976).
[14]I. A. Blech, J. Electrochem. Soc. **131**, C325 (1984).
[15]I. A. Blech and K. L. Tai, Appl. Phys. Lett. **30**, 387 (1977).
[16]I. A. Blech, Acta Mater. **46**, 3717 (1998).
[17]R. Kirchheim, Acta Metall. Mater. **40**, 309 (1992).
[18]L. C. Bassman, *Modeling of Stress-Mediated Self-Diffusion in Polycrystalline Solids* (Stanford University, Palo Alto, CA, 1999).
[19]I. A. Blech, J. Appl. Phys. **47**, 1203 (1976).
[20]M. Lin and C. Basaran, Comput. Mater. Sci. **34**, 82 (2005).
[21]M. E. Sarychev, Y. V. Zhitnikov, L. Borucki, C. L. Liu, and T. M. Makhviladze, J. Appl. Phys. **86**, 3068 (1999).
[22]J. Gomez and C. Basaran, Int. J. Solids Struct. **42**, 3744 (2005).
[23]C. Basaran, H. Tang, and S. Nie, Proceedings of the 55th Electronic Components and Technology Conference, 2005 (unpublished).
[24]A. Dasgupta and J. M. Hu, IEEE Trans. Reliab. **41**, 489 (1992).
[25]H. Tang and C. Basaran, Int. J. Constr. Inf. Technol. **10**, 235 (2001).
[26]B. P. Kashyap and G. S. Murty, Mater. Sci. Eng. **50**, 9 (1981).
[27]H. D. Solomon, Brazing & Soldering, **11**, 68 (1986).
[28]T. Sayama, T. Takayanagi, and T. Mori, American Society of Mechanical Engineers, EEP, 1999.
[29]C. Basaran and Y. Wen, J. Electron. Packag. **125**, 426 (2003).
[30]E. W. Hart, Acta Metall. **5**, 597 (1957).
[31]P. Singh and M. Ohring, J. Appl. Phys. **56**, 899 (1984).
[32]E. O. Hall, Proceedings of the Physical Society, London, 1951 (unpublished).
[33]H. Conrad, Acta Metall. **11**, 75 (1963).
[34]S. G. Tresvyatskii, Strength Mater. **3**, 1320 (1971).
[35]C. R. Siviour, S. M. Walley, W. G. Proud, and J. E. Field, J. Phys. D: Appl. Phys. **38**, 4131 (2005).
[36]J. T. Busby, M. C. Hash, and G. S. Was, J. Nucl. Mater. **336**, 267 (2005).
[37]C. Basaran and J. Jiang, Mech. Mater. **34**, 349 (2002).
[38]R. Balzer and H. Sigvaldason, Phys. Status Solidi B **92**, 143 (1979).
[39]B. Z. Hong, "Thermal fatigue analysis of a Cbga package with lead-free solder fillets," in Thermal and Thermomechanical Phenomena in Electronic Systems, 1998 ITHERM '98, The Sixth Intersociety Conference on, pp. 205–211 1998.
[40]Z. Chen, Y. Shi, Z. Xia, and Y. Yan, J. Electron. Mater. **32**, 235 (2003).
[41]M. Lin, *A Damage Mechanics Framework for Electromigration Failure* (University at Buffalo, State University of New York, New York, 2006).
[42]V. B. Fiks, Fiz. Tverd. Tela (Leningrad) **6**, 2307 (1964).
[43]Y. C. Chuang and C. Y. Liu, Appl. Phys. Lett. **88**, 174105 (2006).
[44]T. Siewert, S. Liu, D. R. Smith, and J. C. Madeni, Properties of Lead-Free Solders 2002 (available from http://www.boulder.nist.gov/div853/lead%20free/part1.html#%201.3).
[45]K. Seelig and D. Suraski, Proceedings of the Electronic Components and Technology Conference, 2000 (unpublished).
[46]D. Suraski and K. Seelig, IEEE Trans. Electron. Packag. Manuf. **24**, 244 (2001).

Downloaded 25 Nov 2008 to 128.205.55.15. Redistribution subject to AIP license or copyright; see http://jap.aip.org/jap/copyright.jsp